Anal Bioanal Chem (2003) 375 : 924–928
DOI 10.1007/s00216-003-1807-3

SPECIAL ISSUE PAPER

A. Gunhold · K. Gömann · L. Beuermann · V. Kempter
G. Borchardt · W. Maus-Friedrichs

Nanostructures on La-doped $SrTiO_3$ surfaces

Received: 29 November 2002 / Revised: 3 December 2002 / Accepted: 16 January 2003 / Published online: 13 March 2003

Abstract $SrTiO_3$(100) single crystals with high donor dopant concentrations (5 at% La) were annealed at 1000 °C for up to 150 h in ultrahigh vacuum (UHV). By applying scanning tunneling microscopy (STM) nanostructures are observed on top of the surface with typical diameters of 20 nm and typical heights of 8 nm. To characterize their electronic structure and chemical composition, the surface was analyzed by metastable impact electron spectroscopy (MIES), ultraviolet photoelectron spectroscopy (UPS), scanning tunneling spectroscopy (STS), and depth profiling Auger electron spectroscopy (AES). Investigations of the stoichiometry suggest that the secondary phases consist of $LaTiO_3$. We present a defect chemistry model which attempts to explain the observed effects.

Keywords $SrTiO_3$ · $LaTiO_3$ · MIES · UPS · AES · STM · STS

Introduction

Strontium titanate ($SrTiO_3$) single crystals have been the subject of numerous investigations because of their relevance in sensor applications, photocatalysis, and as a substrate for high-T_c superconductors [1, 2, 3, 4, 5]. $SrTiO_3$ crystallizes in the cubic perovskite structure with a lattice constant of 3.9 Å and formal ionic charges of Sr^{2+}, Ti^{4+}, and O^{2-}. In the [001] direction the crystal consists of alternating TiO_2 and SrO layers. Therefore only two charge-neutral types of termination are possible: SrO and TiO_2. One would expect both types to be found as top layer, but annealing the polished surface in ultrahigh vacuum results predominantly in a TiO_2 termination [6, 7, 8, 9].

Thermal treatment under oxidizing conditions (air or oxygen atmosphere) leads to the formation of SrO-enriched phases on top of the surface [5, 10, 11, 12, 13, 14]. The underlying process leading to the Sr enrichment is discussed within the framework of point defect chemistry formalism.

The crystals were grown under reducing conditions. On annealing they are oxidized, the number of oxygen vacancies and dislocated electrons is strongly reduced, and the donor dopant compensation mechanism changes to Sr vacancy compensation leading to the diffusion of Sr vacancies into the crystal [15, 16]. The excess Sr segregates to the surface and is incorporated in Ruddlesden–Popper phases ($SrO{\cdot}nSrTiO_3$) in the near surface region and SrO_x phases on top of the surface [14]. The extent of phase formation increases with the dopant concentration.

In contrast, annealing 0.1 at% La-doped $SrTiO_3$ single crystals in UHV leads to the formation of Ti_2O_3 islands on top of the surface by reducing Ti^{4+} partly to Ti^{3+} [17]. These islands are found to agglomerate to large islands during prolonged heating with typical sizes of several µm. It is the aim of this work to extend the investigations to highly doped $SrTiO_3$(100) surfaces heated under reducing conditions in ultrahigh vacuum combining spectroscopic and microscopic methods.

Experimental

The measurements were performed in three different apparatuses: metastable impact electron spectroscopy (MIES) and ultraviolet photoelectron spectroscopy (UPS HeI) were executed in an UHV chamber with a base pressure of $2{\times}10^{-11}$ mbar. It contains a He^*/HeI source with a time-of-flight technique to separate the primary He^* (MIES) and HeI (UPS) beam prior to the interaction with the surface. MIES and UPS spectra are collected simultaneously in a hemispherical analyzer (VSW HA 100) with a resolution of 250 meV under normal emission within 100 s [18]. The angle of incidence for the mixed He^*/HeI beam is 45°. MIES and UPS provide information about the electronic structure, more precisely about the surface density of states (SDOS) and the bulk density of states (BDOS), respectively. The thermal kinetic energy of the metastable He^*

A. Gunhold (✉) · L. Beuermann · V. Kempter · W. Maus-Friedrichs
Institut für Physik und Physikalische Technologien
der TU Clausthal,
Leibnizstrasse 4, 38678 Clausthal-Zellerfeld, Germany
e-mail: anissa.gunhold@tu-clausthal.de

K. Gömann · G. Borchardt
Institut für Metallurgie der TU Clausthal,
Robert-Koch-Strasse 42, 38678 Clausthal-Zellerfeld, Germany

atoms, mostly $He^*(2^3S)$ state, is not sufficient to penetrate into the surface. The resulting electron emission is based on the interaction of the $He^*(1s)$ wavefunctions with the outermost part of the wavefunctions of the surface. Details concerning the He–surface interaction are published in reviews by Morgner [19] and Harada et al. [20]. Thus, MIES is an extremely surface-sensitive technique. The MIES and UPS spectra were displayed as a function of the electron binding energy referring to the Fermi level (E_F), although this is ambiguous for MIES spectra not resulting from the Auger de-excitation (AD) process [18].

Auger electron spectroscopy (AES) was performed in a Perkin–Elmer PEM 595 Auger microprobe equipped with an Ar ion sputter gun for depth profile analysis. It allows spot analysis with a lateral resolution of 1 µm. The AES depth profiles shown here were weighted by the respective sensitivity factors of Sr, Ti, O, and La and yield information on the chemical composition of the restructured surface. The sputter rate was calibrated by using a certified 1000 Å thick Ta_2O_5 layer on top of a Ta sample.

Scanning tunneling microscopy (STM) and spectroscopy (STS) measurements were carried out using an Omicron AFM/STM attached to a third UHV system with a base pressure of 4×10^{-10} mbar in its microscope chamber and below 1×10^{-9} mbar in the main chamber used for annealing. STM was used to investigate the changes of the surface topography during the thermal treatment. STS in combination with STM provides laterally resolved information on the occupation of the surface states, thus allowing to investigate the electrical conductivity. STS is restricted to a range of about ±4 eV around the Fermi level. The combination of STM/STS and MIES/UPS provides microscopic and spectroscopic information over a wide range of binding energies.

Polished 5 at% lanthanum-doped $SrTiO_3(100)$ single crystals (Crystec, Germany) with a size of $10\times10\times1$ mm^3 for the spectroscopic measurements and $5\times5\times0.5$ mm^3 for the microscopic measurements were investigated. To remove surface contaminations completely the crystals were heated for up to 20 h at 700 °C both in the MIES and the STM chamber. The target temperature was in both experiments monitored with an Impac IGA 120 pyrometer, rendering a temperature reproducibility between the different apparatuses of ±10 °C. The AES measurements were performed on crystals being annealed in the MIES/UPS system. Although the sample transfer was performed immediately, this most likely causes surface contaminations during the ex situ transport. The contamination however does not affect the depth profile analysis, as it is restricted to the top layer.

During all heating experiments inside the MIES/UPS apparatus, molybdenum targets were mounted opposite to the sample surface at a distance of about 3 cm. Subsequent Auger analysis of these targets showed adsorbed Ti. Sr could not be found. We are not able to quantify the amount of the sublimated Ti.

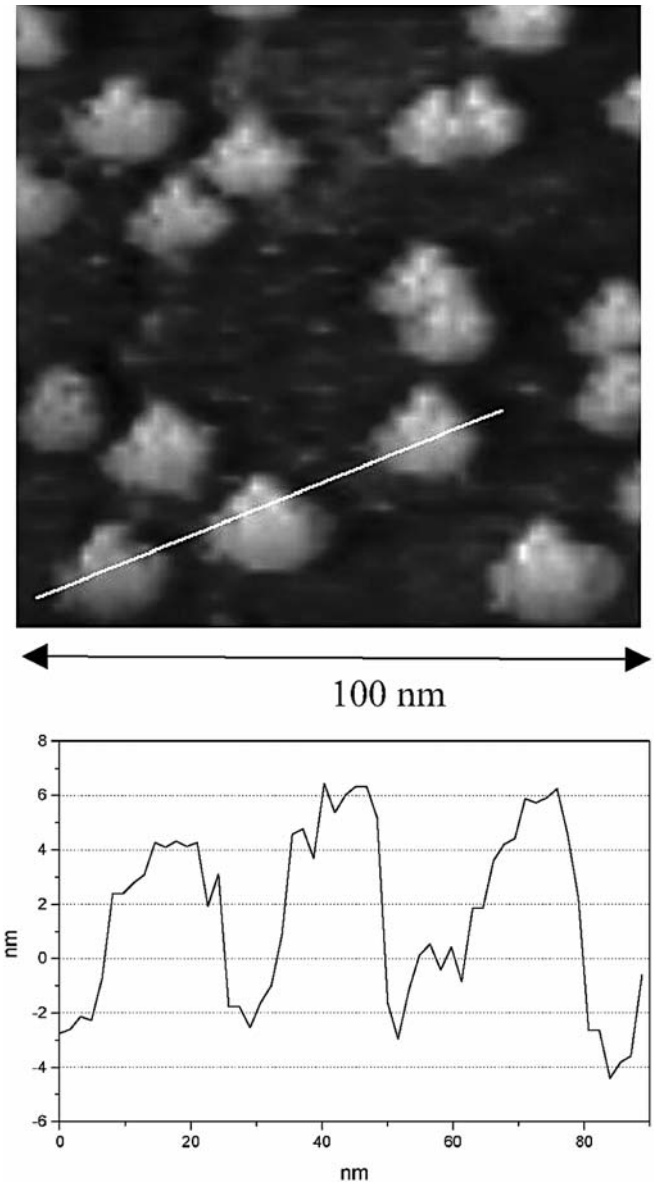

Fig. 1 STM image (100×100 nm^2) of 5 at% La-doped $SrTiO_3(100)$ annealed at 1000 °C for 150 h; gap voltage –1 V/tunneling current 0.5 nA. The graph shows the line profile corresponding to the *white line* in the image

Results

Figure 1 shows a STM image (100×100 nm^2) of the $SrTiO_3$ surface, heated at 1000 °C for 150 h together with a line scan. The surface is covered by a large number of islands with typical diameters of 20 nm and heights of 8 nm which are randomly distributed over the entire surface. In contrast to low dopant concentrations, the nanostructures on single crystals with high dopant concentration do not agglomerate even after heating for 150 h. The surface is covered with islands to about 30%. At shorter heating durations the islands have comparable sizes but their number is smaller.

Figure 2 shows a second STM picture (10×10 nm^2) of the surface region between the islands. Numerous steps are visible with step heights of 2, 4, and 8 Å, corresponding well to 0.5, 1, and 2 lattice spacings of $SrTiO_3$ in the [001] direction. From our current results the domain structures like the flat (1×2) and (2×1) domains reported recently by Erdman et al. on $SrTiO_3(100)$ (99.95% pure) surfaces annealed at 950–1000 °C in an oxygen flow [21] could not be found on crystals heated under reducing conditions. This is likely due to the different atmospheres during the annealing processes.

Figure 3 shows the AES depth profile analysis of this sample. The lateral resolution of the AES is not sufficient to separate the nanostructures and the surrounding surface region. Hence, considering the above results on average island coverage and heights, the first 8 nm of the depth profile should contain contributions from the islands to about 30% and from the uncovered surface to about 70%. The very high O and low Sr and Ti values at the surface

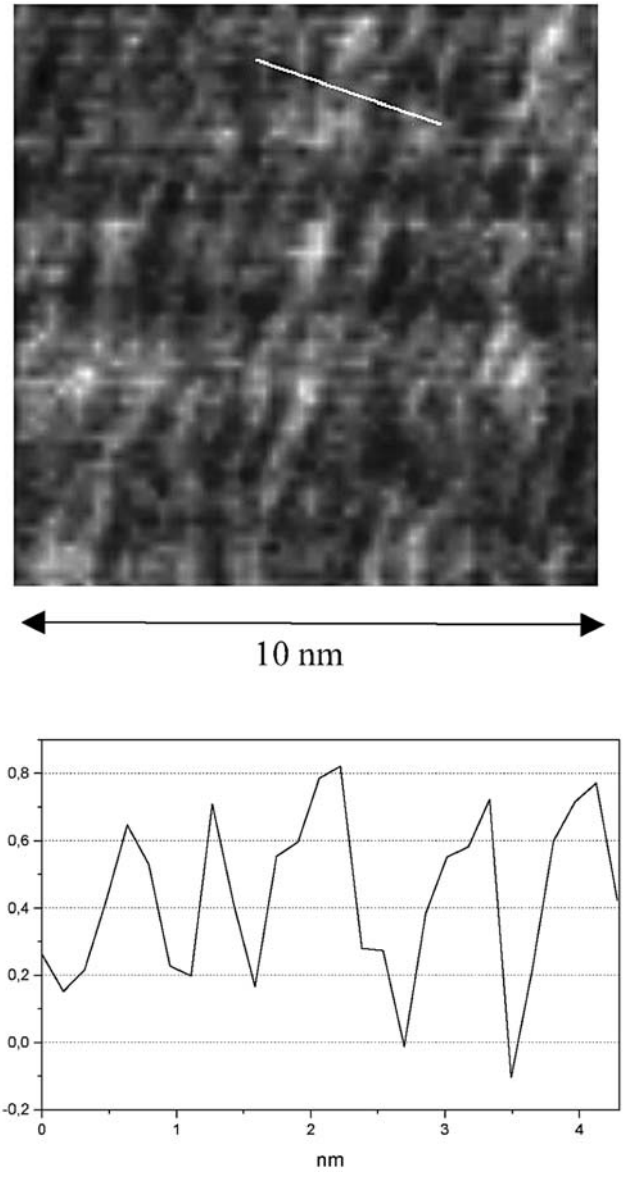

Fig. 2 STM image (10×10 nm^2) of 5 at% La-doped $SrTiO_3$(100) annealed at 1300 °C for 25 h; gap voltage –0.1 V/tunneling current 0.5 nA. The graph shows the line profile corresponding to the *white line* in the image

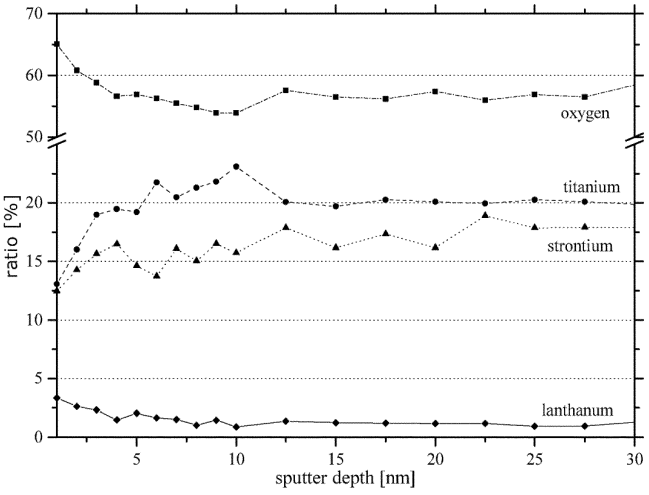

Fig. 3 AES depth profile analysis of 5 at% La-doped $SrTiO_3$(100) annealed at 1000 °C for 72 h

are presumably related to the contributions of oxygen-containing surface contaminants like CO_2 due to the ex situ sample transport. Below 10 nm the depth profile shows an almost constant composition which is close to the starting bulk composition of $Sr_{0.95}La_{0.05}TiO_3$. Thus, only the region between 2 and 10 nm of the depth profile will be discussed here. The Ti concentration increases from 16 at% at 2 nm to 23 at% at 10 nm. La and O show a contrary behavior. La decreases from 3.3 to 1 at%, and O from 61 to 54 at%. The Sr concentration varies between 14 and 16.5 at% but shows no clear behavior.

The MIES and UPS spectra in Fig. 4 show the same surface heated at 1000 °C for different durations as indicated with the spectra. The surface work function, which can be derived from the low energy onset in the UPS spectra, corresponds to 2.7 eV. In addition to the secondary electron contributions beyond a binding energy (E_B) of 10 eV, the MIES spectrum of $SrTiO_3$(100) surfaces is mainly caused by an Auger neutralization (AN) process involving O2p and Ti3d electrons [22]. The Ti^{3+}3d species form a rather narrow band, so the MIES spectrum between 9 eV ≤ E_B ≤ 4 eV is similar to an AD spectrum, but shifted towards higher binding energies by 1.2 eV. In order to compare MIES, UPS, and STS the MIES spectra in Fig. 4 are shifted towards lower binding energies by this value. With the exception of the contributions between 3 eV and 0 eV, the spectra are similar to MIES and UPS [22, 23] spectra of $SrTiO_3$(100) surfaces. The prominent features around E_B=5.2 eV in MIES and E_B=5.0 eV and 7.1 eV in UPS are produced by the electron emission from O(2p). Additional small peaks are observed at E_B=0.5 eV in MIES and E_B=1.0 eV in UPS. These features are caused by the electron emission from the islands.

Figure 5 shows STS spectra (I/V and dI/dV) of the islands and of the surrounding uncovered surface compared to a clean and undoped $SrTiO_3$(100) surface. Similar spectra are found for all investigated 5 at% $SrTiO_3$(100) surfaces annealed under reducing conditions for different durations. A band gap of 3.2 eV is observed and its Fermi level is pinned to the conduction band minimum due to its intrinsic Schottky defects [21]. The small peaks between about –0.1 eV and –2 eV are apparently caused by occupied Ti3d orbitals resulting from defects like reduced Ti lattice ions (Ti'_{Ti}) [22]. Nevertheless, the conductance spectrum clearly indicates that this surface is insulating because the curve approximates zero at the Fermi level (U=0). The spectrum of the surface between the islands also shows an insulating character (band gap of about 3.6 eV). In contrast, STS of the islands yields different behavior due to the corresponding curve being non-zero at the Fermi level. We therefore assume that the weak MIES peak observed at E_B=0.5 eV for this sample (see Fig. 4b) is caused by the density of states (DOS) of the islands.

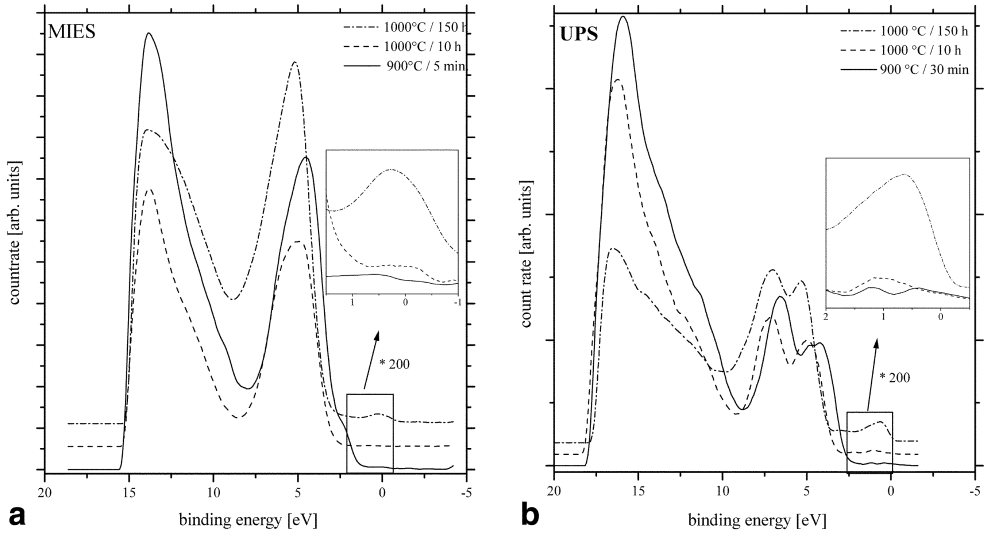

Fig. 4 MIES (**a**) and UPS (**b**) spectra of 5 at% La-doped $SrTiO_3$(100) annealed at 1000 °C for different durations as indicated

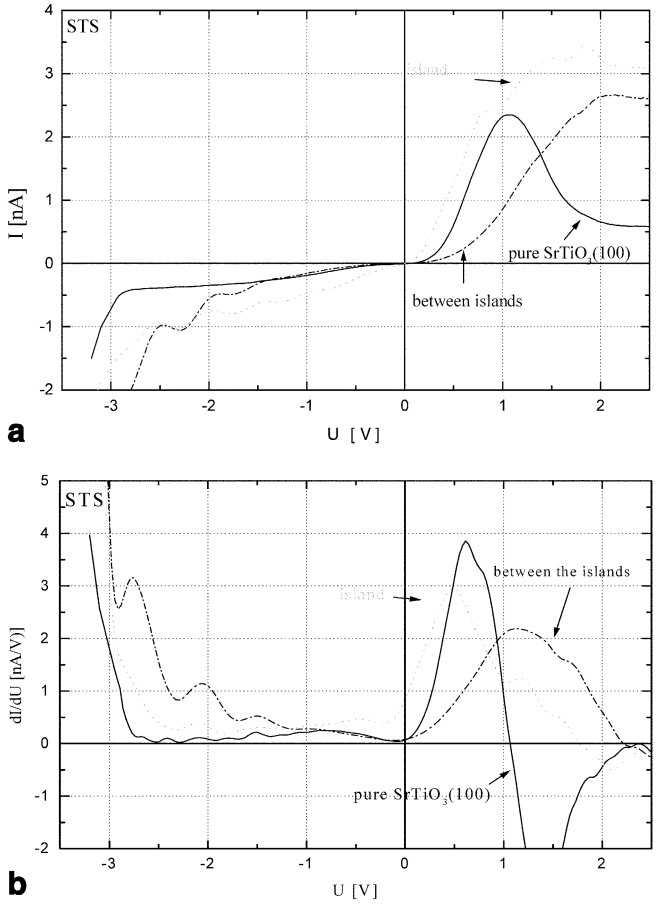

Fig. 5 STS (I/V) (**a**) and (dI/dV) (**b**) spectra of different surface regions and nanostructures of the annealed 5 at% La-doped $SrTiO_3$(100) crystal shown in Fig. 1. A STS spectrum of the surface of clean, unheated, and undoped (pure) $SrTiO_3$(100) is shown for comparison

Discussion

The formation of Ti_2O_3 islands on 0.1 at% La-doped $SrTiO_3$(100) surfaces under reducing conditions has been discussed previously [17]. During the heating procedure oxygen vacancies are created at the surface partly leading to the reoccupation of Ti3d orbitals, which are found in the UPS spectra. These vacancies cannot be refilled due to the low oxygen partial pressure $p(O_2)$ of the UHV. This leads to the formation of Ti vacancies and Ti_2O_3 islands at the surface. The islands agglomerate to large islands and show a metallic-like behavior [17].

Aside from the contributions just below the Fermi level, the MIES and UPS spectra of the 5 at% La-doped crystals investigated here resemble the ones of unheated $SrTiO_3$(100). This means that the observed small contributions just below E_F are most probably related to the islands. These peaks are, as well as the metallic-like character determined with STS, quite weak compared to the observations on weakly doped $SrTiO_3$(100) surfaces. These show strong peaks below E_F even for lower island coverage that were attributed to the formation of Ti_2O_3 [17]. Hence, the islands on the 5 at% La doped samples have a different, most probably less conducting electronic structure.

The AES depth profile shows a Sr depletion in the top 10 nm corresponding to the observed island heights of typically 8 nm. If the stoichiometry of $SrTiO_3$ is largely preserved and the surface is covered to about 30% by islands which do not contain Sr, the Sr concentration obtained in the top 10 nm should be about 14 at%, corresponding well to the measured values. We therefore conclude that the observed La enrichment is due to the La incorporation into the islands. From the depth distribution of La, O, and Ti we gather that the outer shell of the islands consists most probably of La, Ti, and O, whereas the core of the islands is composed of reduced TiO_x, similar to the findings on less doped $SrTiO_3$.

Four stable stoichiometric compounds are known in the La–Ti–O system [21]:

$La_{2/3}TiO_3$, $LaTiO_3$, $La_2Ti_2O_7$, and $La_5Ti_5O_{17}$

Ti^{3+}3d occurs only in $LaTiO_3$. In all other stoichiometries Ti^{4+} is found. It is likely to attribute the STS and MIES results presented above, showing electron density around the Fermi level, to occupied Ti^{3+}3d orbitals. This suggests that

the observed islands consist at least partly of the perovskite $LaTiO_3$, which possesses a crystal structure similar to $SrTiO_3$ with a lattice constant of 3.92 Å instead of 3.91 Å [24]. We are not aware of valence band spectra of $LaTiO_3$ but we assume the DOS to be quite similar to $SrTiO_3$ because of the same lattice structure with the exception of the occupied Ti3d orbitals. This would explain why the MIES spectra beyond E_B=3 eV are quite similar to $SrTiO_3$(100) spectra although about 30% of the surface are covered by $LaTiO_3$.

The formation of $LaTiO_3$ islands can be discussed using a defect chemistry model: the Schottky equilibrium requires the product of oxygen and strontium vacancy concentration to be constant at a given temperature:

$$\left[V_O^{\bullet\bullet}\right]\left[V''_{Sr}\right] = c_1 \quad (1)$$

The intercalation of the La dopants may be written as:

$$2La_2O_3 + 3Sr_{Sr}^{x} \rightarrow 2La_{Sr}^{\bullet} + 3SrO \uparrow + V''_{Sr} \quad (2)$$

$\left[Sr_{Sr}^{x}\right]$ remains approximately constant. So the law of mass action can be deduced as:

$$\left[La_{Sr}^{\bullet}\right]^2\left[V''_{Sr}\right] = c_2 \quad (3)$$

During annealing in UHV, oxygen vacancies are produced which cannot be refilled from the surrounding atmosphere. Equation 1 requires the Sr vacancy concentration to decrease accordingly. Because no free Sr is available, this is not feasible. But alternatively, following from the combination of Eqs. 1 and 3, the increase of the O vacancy concentration may also be compensated by an increase in the La concentration.

$$\frac{\left[V_O^{\bullet\bullet}\right]\left[V''_{Sr}\right]}{\left[La_{Sr}^{\bullet}\right]^2\left[V''_{Sr}\right]} = \frac{\left[V_O^{\bullet\bullet}\right]}{\left[La_{Sr}^{\bullet}\right]^2} = \frac{c_1}{c_2} = \text{constant} \quad (4)$$

This explains the La segregation in highly doped crystals. As annealing for longer than 150 h does not lead to further changes in the electronic or geometric structure of the surface, we assume that the surface is at that time up to a sufficient depth in equilibrium with the atmosphere.

A second process to compensate for the oxygen vacancies and reduce the electron concentration in the crystal is to reduce Ti^{4+} cations:

$$Ti_{Ti}^{x} + ne' \rightarrow Ti_{Ti}^{n'}\ (n = 1, 2, 3) \quad (5)$$

$$Ti_{Ti}^{x} + 4 \cdot e' \leftrightarrow Vi''''_{Ti} + Ti \uparrow \quad (6)$$

This could explain the desorption of Ti from the surface as well as the reduced Ti phases found in islands on weakly doped crystals as well as in the island cores on the strongly doped crystals.

The observation that the islands do not agglomerate even after annealing for 150 h indicates that the island formation may have started at surface defects fixed in their positions. Further experiments will be performed addressing this question.

Summary

Under reducing conditions (total pressure below 1×10^{-8} mbar) on 5 at% La-doped $SrTiO_3$(100) single crystal surfaces the formation of islands is observed at temperatures between 1000 °C and 1300 °C. These islands have typical diameters of 20 nm and heights of 8 nm.

Furthermore, an enrichment of La and Ti is found at the surface which can be attributed to the islands. Oxygen vacancies produced on top of the TiO_2-terminated $SrTiO_3$(100) surfaces segregate into the crystal. These vacancies are compensated by the segregation of La to the surface and the reduction of Ti. Excess Ti and La form islands at the surface which most probably consist of $LaTiO_3$ at the surface and reduced Ti–O phases in the core. These islands do not agglomerate even after prolonged heating. Most probably they are fixed at surface defects. Also the desorption of Ti from the surface is found.

Acknowledgements Financial support by the Deutsche Forschungsgemeinschaft under contracts MA 1893/2 and BO 532/47 is gratefully acknowledged. The authors thank P. Cyris who performed the AES analyses.

References

1. Ravikumar V, Wolf D, David VP (1995) Phys Rev Lett 74:174
2. Stäuble-Pümpin B, Ilge B, Matijasevic VC, Scholte PMLO, Steinfort AJ, Tuinstra F (1996) Surf Sci 369:313
3. Matsumoto T, Tanaka H, Kawai T, Kawai S (1992) Surf Sci Lett 278:L153
4. Liang Y, Bonell DA (1993) Surf Sci Lett 285:L510
5. Szot K, Speier W, Herion J, Freiburg Ch (1997) Appl Phys A 64:55
6. Castell MR (2002) Surf Sci 505:1
7. Castell MR (2003) Surf Sci (in press)
8. Hirata A, Saiki K, Koma A, Ando A (2002) Surf Sci 319:267
9. Lopez A, Heller T, Bitzer T, Chen Q, Richardson NV (2001) Surf Sci Lett 494:L811
10. Szot K, Speier W (1999) Phys Rev B 60:5909
11. Szot K, Speier W, Breuer U, Meyer R, Szade J, Waser R (2000) Surf Sci 460:112
12. Wei H, Beuermann L, Helmbold J, Borchadt G, Kempter V, Lilienkamp G, Maus-Friedrichs W (2001) J Eur Ceram Soc 21:1677
13. Wei H, Maus-Friedrichs W, Lilienkamp G, Kempter V, Helmbold J, Gömann K, Borchardt G (2002) J Electroceram 8:221
14. Gunhold A, Gömann K, Beuermann L, Frerichs M, Borchardt G, Kempter V, Maus-Friedrichs W (2002) Surf Sci 507–510: 447
15. Moos R, Härdtl K-H (1997) J Am Ceram Soc 80:2549
16. Meyer R, Helmbold J, Borchardt G, Waser R (2003) Phys Rev Lett (in press)
17. Gunhold A, Beuermann L, Frerichs M, Gömann K, Kempter V, Borchardt G, Maus Friedrichs W (2003) Surf Sci (in press)
18. Brause M, Braun B, Ochs D, Maus-Friedrichs W, Kempter V (1998) Surf Sci 398:184
19. Morgner H (2000) Adv At Mol Opt Phys 48:387
20. Harada Y, Masuda S, Ozaki H (1997) Chem Rev 97:1897–1951
21. Williams T, Schmalle H, Reller A, Lichtenberg F, Widmer D, Bednorz G (1991) J Solid State Chem 93:534
22. Maus-Friedrichs W, Frerichs M, Gunhold A, Krischok S, Kempter V, Bihlmayer G (2002) Surf Sci 515:499–506
23. Henrich VE, Cox PA (1994) The surface science of metal oxides. Cambridge University Press, Cambridge
24. Wyckoff RWG (1964) Crystal structures vol 2, 2nd edn. Wiley, New York
25. Erdman N, Poeppelmeier KR, Asta M, Warschkow O, Ellis DE, Marks LD (2002) Nature 519:55